Revista de la Academia Colombiana de Ciencias Exactas, Físicas y Naturales
49(193):714-727, octubre-diciembre de 2025. doi: https://doi.org/10.18257/raccefyn.3256

Physical sciences

Original article

AI-Guided Discovery of Chiral Kagome Materials: Linking Wyckoff Symmetry, Oxidation States, and Electronic Topology

Descubrimiento asistido por IA de materiales Kagome quirales: relación entre simetría de Wyckoff, estados de oxidación y topología electrónica

Aldo H. Romero

Department of Physics and Astronomy, West Virginia University, Morgantown, USA

Inaugural article as correspondent member of the Academia Colombiana de Ciencias Exactas Físicas y Naturales

Abstract

We present a systematic screening of binary compounds crystallizing in chiral space group $P6_222$, targeting candidate chiral Kagome metals. By combining Wyckoff-resolved site analysis with Shannon ionic radii and oxidation states, we link atomic size/valence to preferred Wyckoff positions—especially the 3*d* site that forms Kagome planes. Across >300 structures, smaller cations favor the 3*d* site, while larger ions occupy peripheral sites (3*c*, 6*j*). Contrasting Ca- vs. Ir-based prototypes reveal divergent magnetic ground states and distinct spin–orbit responses despite identical symmetry, underscoring how local coordination governs electronic topology. These results provide design rules for engineering new chiral Kagome materials that rival canonical systems such as Fe_3Sn_2 and CoSn.

Keywords: Kagome, chirality, Wyckoff positions, topological materials, machine learning.

Resumen

En este paper presentamos una búsqueda sistemática de compuestos binarios que cristalizan en el grupo espacial quiral $P6_222$ con el objetivo de identificar nuevos metales Kagome quirales. Mediante la combinación de un análisis de posiciones de Wyckoff con radios iónicos de Shannon y estados de oxidación, establecemos correlaciones entre el tamaño atómico, la valencia y la ocupación preferencial de sitios cristalográficos, particularmente del sitio 3*d* que forma las redes Kagome. El análisis de más de 300 estructuras revela que los cationes de menor tamaño tienden a ocupar preferentemente las posiciones 3*d* d, mientras que los iones de mayor tamaño se ubican en sitios periféricos (3*c*, 6*j*). Los prototipos basados en calcio e iridio exhiben estados magnéticos diferenciados y respuestas contrastantes al acoplamiento espín–órbita, a pesar de compartir la misma simetría cristalina, lo cual evidencia el papel determinante de la coordinación local en la topología electrónica resultante. Estos hallazgos proporcionan principios de diseño fundamentales para la síntesis dirigida de nuevos materiales Kagome quirales con propiedades comparables a las de Fe_3Sn_2 y CoSn.

Palabras clave: Kagome, quiralidad, posiciones de Wyckoff, materiales topológicos, aprendizaje automático.

Introduction

Advances in quantum computing, neuromorphic logic, and low-loss photonics all hinge on discovering crystals whose electronic or magnetic ground states are finely tuned by symmetry (**Newnham,** 2004; **Powell & Powell,** 2010; **Prakash & Wei,** 2014). In theory, that structural search for three dimensional materials reduces to a combinatorial exercise: populate the Wyckoff positions of the 230 space groups with atomic species, generate a metrically valid lattice, then ask whether the resulting structure is both chemically

Citation: Romero AH. AI-Guided Discovery of Chiral Kagome Materials: Linking Wyckoff Symmetry, Oxidation States, and Electronic Topology. Revista de la Academia Colombiana de Ciencias Exactas, Físicas y Naturales. 49(193):714-727, octubre-diciembre de 2025. doi: https://doi.org/10.18257/raccefyn.3256

Editor: Jairo Roa Rojas

Corresponding autor:
Aldo Humberto Romero Castro;
correo@correo.edu.co

Received: July 16, 2025
Accepted: August 14, 2025
Published on line: October 14, 2025

sensible and energetically competitive. Classical enumerators such as PyXtal already automate the first step (**Fredericks *et al.,*** 2021), inserting sites one Wyckoff position at a time and rejecting duplicates by group–subgroup checks (**Ivantchev *et al.,*** 2000). Recent generators—including WyFormer (**Kazeev *et al.,*** 2025) and WyCryst—package (**Zhu *et al.,*** 2024) the same symmetry rules inside artificial intelligence (AI) deep generative models, compressing a unit cell into a few dozen discrete tokens and ensuring that every candidate obeys its parent space-group operations by construction.

The bottleneck is no longer the enumeration itself, but the rate at which those candidates can be triaged once cell sizes climb to 40–60 atoms. A brute-force density-functional-theory (DFT) relaxation of that many heavy cells would stall even on a national supercomputer. Two large-scale efforts have shown how machine learning removes the choke-point. DeepMind's GNoME couples graph-neural-network (GNN) surrogates to on-the-fly DFT (**Merchant *et al.,*** 2023); the surrogate filters roughly twenty million symmetry-compliant inputs per day and schedules only the top fraction for ab-initio confirmation, ultimately identifying 381,000 new hull-stable compounds. At the same time, major initiatives like the ALEXANDRIA project, led by M.A.L. Marques at Ruhr-Universität Bochum, are using artificial intelligence to accelerate materials discovery. ALEXANDRIA has performed over five million full quantum mechanical simulations using density functional theory (DFT), a standard method for calculating the energy and atomic structure of materials (**Schmidt *et al.,*** 2024). To identify promising new materials, the project uses a specialized machine learning model called a crystal-graph attention network, which predicts whether a structure is likely to be stable by comparing its energy to that of the most stable known phases—a reference known as the convex hull. Remarkably, this method maintains an energy accuracy within 0.1 eV per atom of the convex hull, even for large and complex structures containing up to fifty atoms (**Schmidt *et al.,*** 2024).

Independent benchmarks, such as the NIST JARVIS-Leaderboard, confirm the accuracy of related models like ALIGNN (Atomistic Line Graph Neural Networks), which are trained on the same data infrastructure. These models now predict formation energies with mean absolute errors below 20 meV per atom and can be executed in milliseconds from within a standard Python notebook (**Choudhary *et al.,*** 2020, 2024; **M. Liu & Meng,** 2024). While ALEXANDRIA is among the largest efforts of its kind, many other groups are developing similar AI-driven tools for materials design.

In the methodology reported here, we merge those ingredients—explicit Wyckoff enumeration, lattice feasibility checks, and a light-weight GNN surrogate—into a workflow that can vet roughly thousands of 40–60-atom prototypes each day on a single eight-GPU node. First, space-group templates are drawn from the International Tables and populated stochastically; steric filters as implemented in PyXtal eliminate (**Fredericks *et al.,*** 2021).

Next, a transfer-learned ALIGNN model scores the raw structures for enthalpy and electronic gap; only the top decile proceeds to full relaxation. Finally, a small self-consistent DFT loop, parallelised over CPUs, validates the survivors and feeds new data back into the training pool, an approach analogous to the active-learning schemes reviewed for universal machine-learning interatomic potentials (uMLIPs), we have used the M3Gnet model (**C. Chen & Ong,** 2022).

The message from this paper is straightforward: crystallographic symmetry collapses an astronomically large search space into a tractable library of Wyckoff graphs; modern graph networks supply the speed to explore that library at industrial scale. By leveraging both, our pipeline delivers chemically diverse, symmetry-correct crystal candidates at a rate that aligns with daily HPC allocations. To demonstrate the workflow, we decided to search over a small binary family over the so-called Kagome lattices.

A Kagome lattice is a two-dimensional web of corner-sharing triangles. Despite its simplicity, this structure is a hotbed of complexity: it frustrates magnetic order, supports flat electronic bands, and gives rise to quantum phenomena such as Dirac and Weyl fermions, correlated magnetism, and unconventional superconductivity (**Wang *et al.,*** 2024; **Yin *et al.,*** 2022). As researchers increasingly combine artificial intelligence with quantum

Revista de la Academia Colombiana de Ciencias Exactas, Físicas y Naturales
49(193):714-727, octubre-diciembre de 2025. doi: https://doi.org/10.18257/raccefyn.3256

physics, the Kagome lattice stands out as a powerful testbed. This lattice—named after the traditional Japanese basket-weaving pattern meaning "basket-eye" (kago = basket, me = eye)—has a rich history rooted in both mathematics and physics. The term was coined by Kodi Husimi in the early 1950s (**Mekata,** 2003), inspired by the trihexagonal tiling seen in Japanese baskets. Its structure—a 2D network of corner-sharing triangles and hexagons—had been known since at least Kepler (1619), who described it as part of uniform plane tilings (a network with the $(3.6)^2$ Archimedes tiling). In the 1950s and 1970s, the Kagome lattice became a key model for geometrical frustration in magnetic systems, revealing a wealth of potential ground states. It was first studied as an idealized platform to understand frustrated magnetism and nontrivial spin arrangements, with foundational models explored by A. Yoshimori, Kaplan, Elliott, Wannier, and Toulouse (**Elliott,** 1961; **Kaplan,** 1961; **Toulouse,** 2008; **Wannier,** 1950; **Yoshimori,** 1959).

In 2D materials, this lattice geometry has garnered considerable attention for its ability to host exotic quantum phenomena such as flat bands, Dirac cones, and topological edge states. Prototypical examples include Fe_3Sn_2, which exhibits anomalous Hall effects and massive Dirac fermions (**Ye *et al.,*** 2018), and CoSn, where Dirac-like dispersions and nodal lines emerge due to the symmetry of the Kagome net (**Z. Liu *et al.,*** 2020). These 2D systems are often treated as layered structures with quasi-2D electron transport, limiting their tunability along the out-of-plane direction. In contrast, three-dimensional (3D) Kagome lattices extend this geometry into a fully interconnected network across all three spatial dimensions, offering a much richer playground for emergent quantum states. 3D Kagome structures can preserve the essential features of their 2D counterparts—such as geometric frustration and Dirac-like crossings—while enabling enhanced structural flexibility, anisotropic bonding, and the possibility of non-symmorphic symmetry elements, such as screw axes and glide planes, that are absent in 2D layers. These features can stabilize a broader array of magnetic orders, topological semimetals, and chiral spin textures. Notably, compounds like Mn_3Sn (hexagonal, noncollinear antiferromagnet) and AV_3Sb_5 (where A = K, Rb, Cs) (**Nakatsuji *et al.,*** 2015; **Ortiz *et al.,*** 2020) exhibit charge density waves, unconventional superconductivity, and intertwined orders arising from 3D Kagome connectivity. The enhanced chemical and crystallographic flexibility of 3D Kagome frameworks also makes them ideal for exploring structure-property relationships, especially in chiral space groups such as $P6_22$, where symmetry-enforced constraints can be exploited for band engineering, topological design, and spin-orbit-driven phenomena. This motivates the search for new 3D Kagome compounds using data-driven and symmetry-aware approaches, such as the one proposed in this study.

On the other hand, some crystal materials are "handed" in the same way a left hand differs from a right. When their atoms line up in a pattern called a chiral lattice (one example is labeled $P6_22$ in crystal symmetry notation), the arrangement cannot be flipped or mirrored to look the same—there is no built-in plane of symmetry (see, for example, an enantiomeric crystal pair in **Figure 1**). That subtle lack of mirror-image symmetry can have outsized consequences: it lets the material twist light, host exotic electronic states, and even mimic the way biological molecules distinguish left from right (**Bousquet *et al.,*** 2024). Because such chiral fabrics are rare in nature, uncovering new ones is a high-value goal for materials discovery. Introducing chirality—an intrinsic sense of "handedness" in a crystal—unlocks a class of remarkable quantum behaviors that aren't possible in ordinary, symmetric materials. First, it can stabilize Weyl fermions, emergent particles that act like massless electrons with a built-in directionality. These exotic excitations behave like tiny sources and sinks of a field known as Berry curvature, which captures how an electron's wavefunction twists through the material's structure (**Zhang *et al.,*** 2021). This built-in "twistiness" leads to topological surface states—unique electronic pathways known as Fermi arcs—that appear only on the material's surfaces and can channel electrons in ways that are highly resistant to scattering (**Hasan *et al.,*** 2017). Such effects do not occur in conventional (non-chiral) systems. In simpler terms, chirality in

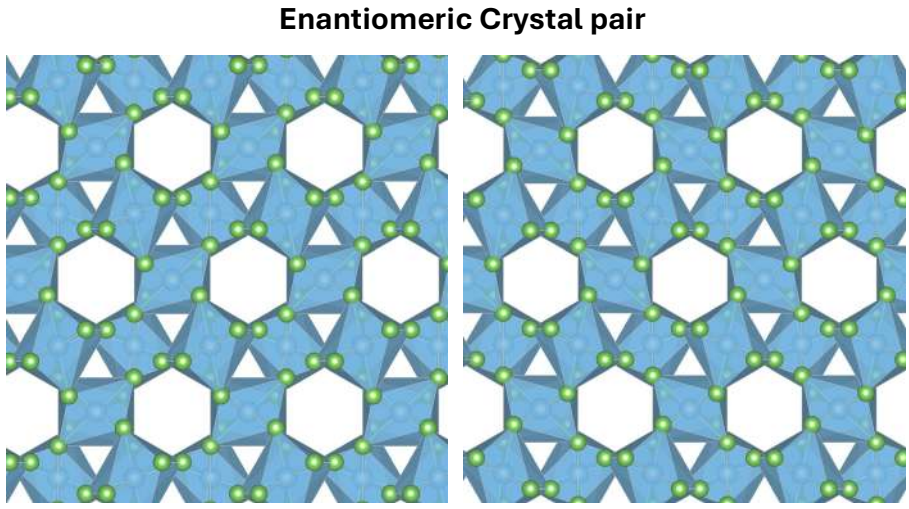

Figure 1. Enantiomeric pair of TiAs structures crystallizing in chiral space groups: left, space group 180; right, space group 181. Both structures share the same stoichiometry and atomic configuration—blue spheres represent Ti atoms, and green spheres represent As atoms—but differ in their crystallographic handedness. The mirror asymmetry between the two structures arises from the opposite screw axes defining each space group, highlighting the emergence of structural chirality even in achiral compositions.

a crystal lattice is like giving it a built-in bias or fingerprint that forces electrons to act differently. The result is emergent quantum behaviors—Weyl particles, hidden "twisted" fields, and special surface highways—that could lead to new low-loss electronics, unusual magnetic or optical effects, and components that behave differently for left- or right-handed crystals (important for sensing or information processing) (**Hasan *et al.,*** 2021; **You *et al.,*** 2023). Now, our application for the workflow presented here is to apply it to a family where there is a small number of materials reported, those which are chiral but also can host Kagome lattices in the atomic motif. Chirality itself also extends to lattice dynamics. Non-centrosymmetric structures support chiral phonon modes that carry angular momentum, which can couple to spin degrees of freedom and give rise to phonon-driven spin transport or magneto-phononic phenomena (**H. Chen *et al.,*** 2019; **Li *et al.,*** 2022). Moreover, structural enantiomorphs in $P6_222$ vs. $P6_422$ offer a natural platform to explore chiral-selective effects such as circular dichroism and magnetochiral anisotropy—critical in nonlinear optics and spintronics (**Bousquet et al.,** 2024).

Among chiral space groups, $P6_222$ (No. 180) is particularly versatile due to its rich set of symmetry-defined atomic sites known as Wyckoff positions **Tasci *et al.,*** 2012. Of the eleven available, four positions—3a, 3b, 3c, and 3d—each form a triangular arrangement that individually supports the geometry of a Kagome lattice. In other words, placing atoms in any one of these positions is enough to generate the Kagome pattern, making this space group especially valuable for designing such lattices in chiral materials. This structural flexibility allows researchers to finely control a material's composition and internal order. By assigning different atomic species to two or three positions, one can tune the stoichiometry, tailor bonding environments, and engineer functional networks—such as magnetic or conductive pathways. Compared to other chiral groups, $P6_222$ offers a significantly broader design space (**Bousquet *et al.,*** 2024). Its multiple interchangeable sites enable the creation of materials with customizable electronic, magnetic, and topological properties, making it a fertile ground for discovering new functional crystals.

A key challenge in designing chiral Kagome materials is choosing the right chemical building blocks. In this study, we restrict our search to binary compounds made from elements up to bismuth (Bi) in the periodic table, focusing specifically on structures

Revista de la Academia Colombiana de Ciencias Exactas, Físicas y Naturales
49(193):714-727, octubre-diciembre de 2025. doi: https://doi.org/10.18257/raccefyn.3256

where the 3d Wyckoff position in space group $P6_222$ is occupied—sufficient on its own to generate the Kagome lattice motif. Future work will expand this approach to explore other Wyckoff positions and more complex ternary compositions. An additional critical factor is the oxidation state, which governs charge balance and electron filling. Stable Kagome structures often depend on precise electron counts; imbalances can disrupt the lattice or suppress quantum effects (**Saini,** 2023; **Zhou *et al.,*** 2024). For this purpose, we considered all reported oxidation states available from the **Los Alamos database Laboratory,** 2025. Notably, early transition metals bring partially filled d-orbitals, which are crucial for magnetism and correlation-driven topological phases (**Negi *et al.,*** 2025; **Yin *et al.,*** 2022).

Our goal is to open a pathway toward the discovery of new materials that merge geometric frustration, chirality, and topological order—a combination at the core of next-generation quantum materials for applications in spintronics, low-power electronics, and quantum information science.

Methodology

The methodology used in this work for the high-throughput discovery of topological quantum materials can be broadly divided into three main phases: (1) structure generation and enumeration, (2) AI-assisted structural relaxation and energy prediction, and (3) property evaluation and final validation, as summarized in **figure 2**. In the first phase, we target a specific crystallographic space group—space group 180 ($P6_322$)—which is chiral and features multiple unique Wyckoff positions (notably 3a–3d), making it ideal for constructing structurally diverse Kagome-like lattices. For each selected combination of atomic species, we go through all possible stoichiometries and ways the atoms could be placed on Wyckoff positions. We use two main rules: (1) no two species can be placed on the same Wyckoff position, and (2) a species can be placed on more than one Wyckoff

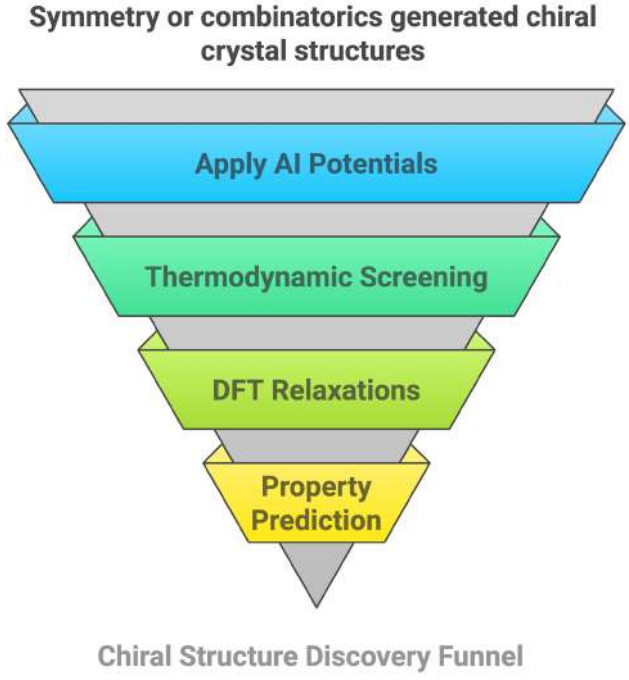

Figure 2. Chiral structure discovery funnel used in this study. The process begins with chiral crystal structures generated through symmetry analysis or combinatorial enumeration. These candidate structures are first filtered using fast surrogate models based on AI interatomic potentials. Surviving structures undergo thermodynamic screening to assess their proximity to the convex hull. Promising candidates are then subject to full DFT relaxations for

position. While doing this, we also check for basic chemical rules, like making sure the oxidation states are balanced and the ionic sizes make sense together. These checks help us avoid unrealistic structures. In future work, we plan to relax these two rules to explore a wider range of possible structures.

To ensure the presence of a Kagome lattice, we explicitly place at least one atomic species on the 3d Wyckoff position in each selected chiral space group. The remaining atoms are distributed across other symmetry-allowed Wyckoff sites in the same space group, respecting site multiplicities and chemical valence considerations. Each assignment is treated combinatorially, producing a broad set of candidate prototype structures. For Wyckoff sites with free positional parameters, coordinates are sampled randomly within physically plausible bounds. To prevent unphysical structures, we enforce interatomic distance constraints, requiring all atom pairs to fall within 0.8 × to 2 × the sum of their van der Waals radii. This constraint avoids both steric clashes and unrealistically sparse packing. Through this procedure, we generate a diverse set of candidate chiral Kagome materials that preserve symmetry, maintain chemical plausibility, and span a broad range of structural motifs.

Figure 3 presents a small set of these symmetry-limited prototypes, showcasing six chiral structures generated within space group 180, each featuring the Kagome arrangement. The illustration emphasizes the variety in Wyckoff positions present in this space group and chemical compositions that arise from the automated enumeration method, highlighting how minor changes in site designation, chemical species or ionic radius can produce unique Kagome structures. The visualized prototypes illustrate the structural landscape sampled during our AI-assisted screening and confirm that the pipeline reliably maintains chirality and Kagome connectivity across various chemistries, where the three fold coordination is maintained by the selected species.

In the second phase, artificial intelligence is used to dramatically reduce computational costs during geometry optimization. Instead of relying entirely on density functional theory (DFT)—which is highly accurate but computationally expensive—we follow the approach of our previous publications, where we apply the universal neural network interatomic potentials M3GNet to relax initial structures. This machine-learned potential is trained on large databases of materials and can predict interatomic forces with good accuracy. Once applied, the crystal structures move closer to their energetic minima. The structures that are predicted to be unstable or far from equilibrium are discarded early, allowing resources to be concentrated on promising candidates.

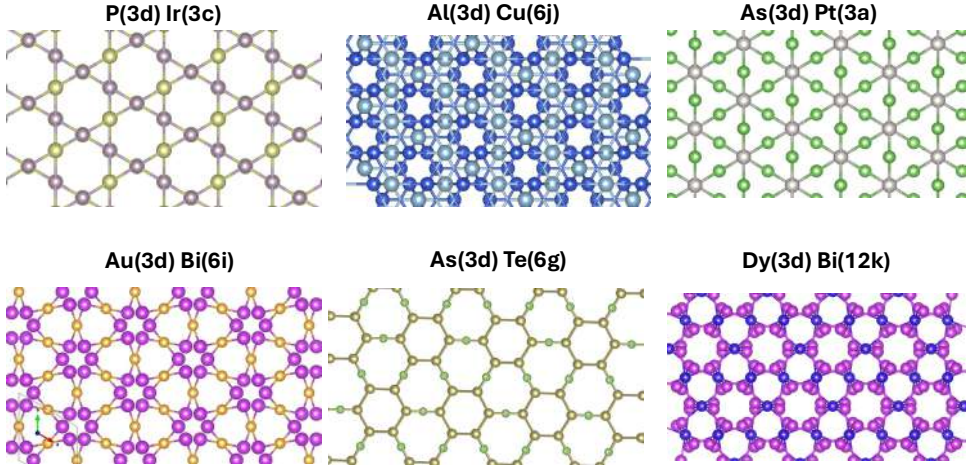

Figure 3. Chiral structure with space group numbewr 180 in a Kagome configuration. These six structures are over the convex hull, atomic compositions and Wyckoff positions are included per each structure.

Revista de la Academia Colombiana de Ciencias Exactas, Físicas y Naturales
49(193):714-727, octubre-diciembre de 2025. doi: https://doi.org/10.18257/raccefyn.3256

Once the initial atomic relaxation of a structure is done, we apply a second stage of AI tools to assess how stable each material is. Specifically, we estimate the formation energy, which tells us how likely it is for a material to form from its constituent elements, and we calculate its distance to the convex hull—a widely used thermodynamic metric that indicates whether a material is more or less stable than any possible combination of other known compounds (**Jain *et al.,*** 2020). If a structure lies on or near this convex hull, it means it is unlikely to break apart into simpler phases and is therefore a strong candidate for experimental synthesis. To make these predictions efficiently, we use machine learning models such as CGCNN (Crystal Graph Convolutional Neural Networks) and similar graph-based algorithms **Xie and Grossman,** 2018. These models treat each material as a network of atoms and bonds, allowing them to learn complex relationships between structure and stability. By relying on these AI-driven surrogate models instead of more computationally intensive quantum mechanical calculations like DFT (Density Functional Theory), we can evaluate millions of hypothetical materials in a matter of weeks rather than several months or years. At this stage, we can also use AI models trained on large materials databases to predict important electronic properties—such as whether the material is metallic or insulating (band gap), whether it might exhibit topological behavior, or whether it could be magnetic. This allows us to rapidly identify the most promising candidates for further, more detailed study.

Finally, only the most promising candidate structures—typically those with formation energies on or within 10 meV/atom of the convex hull—are selected for full DFT relaxation and detailed characterization. For this step, we employed the VASP electronic structure package **Kresse and Furthmüller,** 1996; **Kresse and Hafner,** 1993. Electrons were treated using ultrasoft pseudopotentials (**Kresse & Hafner,** 1994; **Kresse & Joubert,** 1999), and for each structure, we performed energy cutoff and k-point mesh convergence to ensure numerical accuracy within 5×10^{-5} eV for the total energy and 5×10^{-3} eV/Å for the forces. These calculations serve to validate the structural, electronic, and topological predictions made in earlier AI-driven screening steps. The fully relaxed crystal structures were visualized using VESTA (**Momma & Izumi,** 2011), and band structure analyses were carried out using PyProcar (**Herath *et al.,*** 2020; **Lang *et al.,*** 2024).

Results

Among the structures we identified with stable energy (<0.01 eV/atom), the Wyckoff 3d position is notably diverse in occupied species. Rather than listing all 60+ elements appearing at 3d, it is more insightful to group them by chemical families and focus on those most frequent. Key observations include:

- Main-group elements (from p-block): Phosphorus (P) leads with 54 occurrences, followed by Be^{+2} (42), As (42), Si (33), In (21), Sn (18), Ge (9), Al, Sb, I, and Cl (6–12 each).
- Alkaline earth and alkali metals: Be and Mg (27), Ca, Sr (6–12).
- Transition metals: Ti (27), Zr (15), V, Hf, Fe, Rh, Ni, Ru, Au, Pd, Pt (3–15 each).
- Rare earths and lanthanides: Gd, Nd, Eu, Ce, Tb, Dy, Ho, Er, Y, Lu, Sm, Tm (3–24 each).
- Halogens & chalcogens: Cl, Br, I, S (6–12 occurrences).

This highlights that P, Be, As, Si, Ti, and Mg—elements not seen in existing databases' 3d site entries—are among the most frequent. In comparison, repositories like Material Project (**Jain *et al.,*** 2013, 2020), AFLOW (**Curtarolo *et al.,*** 2012), and COD have recorded only 15 binaries with 3d atoms—limited to 10 species (Ce, Cr, Hf, Mo, Nb, Ni, Sc, Ta, V, and W). Our high-throughput search nearly doubles that diversity, uncovering new chemistries in overlooked chemical families.

The reason lies in chemical compatibility with site symmetry. The 3d position imposes threefold planar coordination, which requires atoms whose oxidation state and bonding fit a triangular environment. In that case, P and As (group 15) often adopt oxidation states

around +3, forming planar trigonal coordination. Be, Mg, Ca, Sr (group 2) readily form +2 ions, fitting well into the coordination shell. Transition metals (Ti, V, Zr) offer partially filled d-orbitals that underpin magnetic or electronic behavior. Rare-earth elements (Gd, Nd, etc.) bring +3 oxidation states and stable ionic sizes conducive to symmetry. Halogens and chalcogens like S, Cl, I, Br appear in unexpected but structurally favorable reduced forms (e.g., –1 or 0).

Previous experimental literature on binary Kagome compounds primarily emphasizes late transition metals (Fe, Co, V) and ternary systems(Fe_3Sn_2, CoSn, V_3Sb_5), with few binaries featuring lighter or rarer species. Our work uncovers a much richer palette—demonstrating that elements across six chemical groups can stably occupy the 3d position when oxidation state and symmetry conditions align. This opens an expanded chemical landscape for chiral Kagome materials, pointing to promising new candidates well beyond those captured in classical databases or reported in existing Kagome studies.

Out of the 11 symmetry-distinct Wyckoff positions available in space group 180, our search yielded stable compounds—those on the convex hull—in 9 of them, with only 3d and 6h remaining unoccupied in this dataset. This broad coverage highlights the structural versatility of the space group. Among the occupied sites, the most frequently occurring elements were platinum (Pt) with 25 occurrences, followed closely by gold (Au) with 23, and bismuth (Bi) and titanium (Ti), each appearing 15 times. These trends suggest a preference for late transition metals and heavier main-group elements in energetically favorable configurations within this chiral space group. Our analysis reveals that lighter cations—Be^{2+}, B^{3+}, Al^{3+}—alongside mid-sized As^{3+}, dominate the 3d Wyckoff site in $P6_222$ structures, appearing hundreds of times within our dataset (see **Figure 4**). These ionic radii (0.13–0.58 Å) are significantly smaller than those typically found in classical transition-metal Kagome systems, suggesting an unexplored region of low-mass, stiff Kagome frameworks. This contrast is instructive: conventional Kagome lattices such as KV_3Sb_5 (Sb^{3-} radius 1.05 Å) and Fe_3Sn_2 involve heavier atoms and partially filled d-orbitals that support correlated magnetism and flat-band electronic

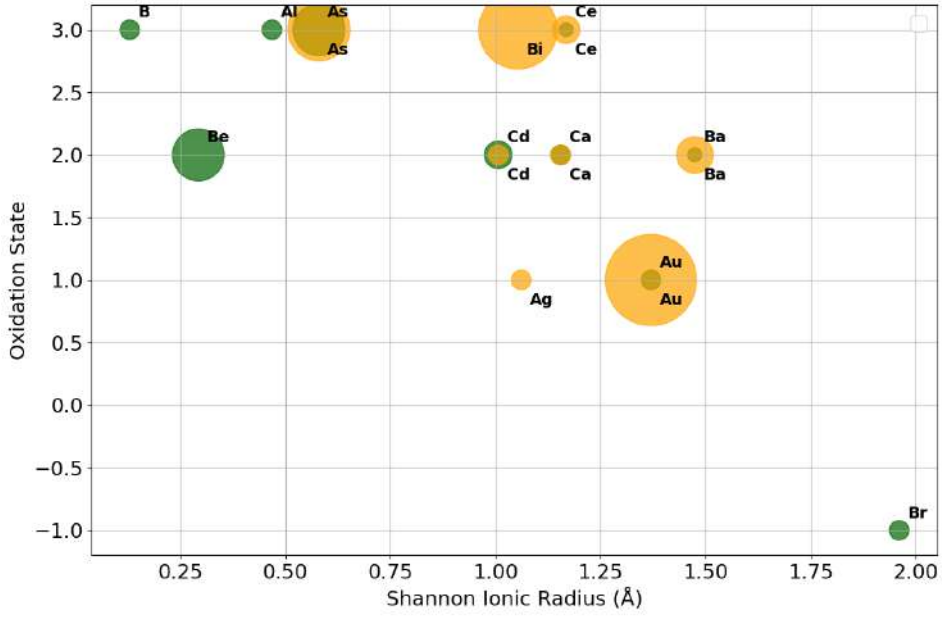

Figure 4. Oxidation state vs. Shannon ionic radius for cations occupying the 3d Wyckoff position (dark green) and other positions (orange) in space group 180 chiral Kagome structures. Marker size scales with the number of occurrences of each element–oxidation state combination across the zero convex hull dataset

Revista de la Academia Colombiana de Ciencias Exactas, Físicas y Naturales
49(193):714-727, octubre-diciembre de 2025. doi: https://doi.org/10.18257/raccefyn.3256

states. In stark contrast, the prevalence of compact cations in 3d motifs hints at novel structural motifs dominated by strong phonon coupling and less by d-electron physics. This can lead to superconductivity, as our analysis of the electron density of states points out that many bands cross the Fermi surface, providing the basic ingredient for electron-phonon coupling. This opens intriguing possibilities for high-frequency lattice dynamics and phonon-mediated topological interactions—an area so far unexplored in Kagome compounds (**Fu *et al.,*** 2025; **Hu *et al.,*** 2024; **Wang *et al.,*** 2024).

Now, in relation to chirality and Kagome lattices, recent studies—such as those on RPt_2B (R = La, Nd)—demonstrate that the 3D Kagome network in such chiral structures fosters magnetic frustration and Kramers-Weyl nodes, with persistent topological features under broken T- and P-symmetries **Ardila-Gutiérrez *et al.,*** 2025. Our findings, which uncover a diverse array of ionic species in the 3d Kagome lattice of SG 180 compounds, raise the possibility that structural chirality might play a key role in stabilizing enantiomorphous Kagome frameworks with unique electronic and phononic signatures. Moreover, chiral systems in Sohncke groups are rare in inorganic solids (< 5% of ICSD entries), but they have proven essential for discovering fascinating phenomena such as chiral phonons and optical activity (**Bousquet *et al.,*** 2024). Therefore, the unexplored space of light-cation Kagome systems in SG 180 may offer fertile ground for discovering novel chiral quantum phases, especially if we pursue both enantiomers experimentally.

To assess the chemical and structural diversity of the generated Kagome dataset, we analyzed the stoichiometry types of all candidate compounds and identified the most prevalent elemental constituents within each group. The most frequent stoichiometry was AB_2, comprising 139 compounds, followed by AB with 67 structures and AB_4 with 9 examples. Notably, the AB_2 compounds were dominated by heavy elements such as gold (Au), platinum (Pt), and arsenic (As), which together suggest a propensity for forming layered or spatially anisotropic structures that support the Kagome motif. The AB stoichiometry also exhibited a rich elemental variety, including platinum, gadolinium (Gd), phosphorus (P), and iridium (Ir), reflecting a mix of transition metals and rare-earth elements potentially conducive to exotic magnetic or electronic behavior. In the smaller AB_4 category, elements such as bismuth (Bi), cesium (Cs), and titanium (Ti) were observed, indicating a limited but chemically distinct subset. Overall, these results confirm that the dataset spans a chemically diverse range of compositions, while subtly favoring late transition metals and heavy p-block elements often associated with strong spin-orbit coupling—features known to stabilize topological and magnetic phases in Kagome frameworks.

It is important to note that the current dataset focuses exclusively on configurations where the Kagome network is stabilized by placing atoms on the 3d Wyckoff position of space group 180, one of four (3a, 3b, 3c, 3d) symmetry-distinct sites capable of supporting this geometry. While this choice introduces a degree of structural bias, it was made to ensure strict geometric preservation of the Kagome motif. Ongoing efforts are expanding this framework to include additional Wyckoff configurations and alternative binary decorations that preserve Kagome topology, which is expected to enhance both the chemical richness and structural diversity of the library. Overall, the current set already spans a broad range of compositions, with a bias toward late transition metals and heavy p-block elements often associated with spin-orbit-driven topological features in chiral Kagome materials.

As a last example of the potential of Chiral Kagome structures, we make a comparison of the electronic properties of PCa_2 and PIr, binaries on the convex hull. In both structures, phosphorus (P) occupies the 3*d* Wyckoff position, playing a central role in forming the Kagome-like network. The difference lies in the metallic partner, Ca in PCa_2 occupies the 6j site, and Ir in PIr occupies the 3c site. This difference is crucial because the site symmetry and atomic number (Z) of Ca and Ir differ significantly, which has direct consequences on the band dispersion, degeneracy, and spin orbit coupling (SOC) response. Without SOC, the band structure of PCa_2 displays several nearly flat bands

near the Fermi level, a hallmark of Kagome physics—potentially linked to localized electronic states or destructive interference from the lattice geometry. In this case, the introduction of SOC does not significantly lift the degeneracies or strongly modify the band topology. This is expected since Ca is a light element (low atomic number) and SOC is weak. The general shape and dispersion remain largely preserved, though small splittings may appear. On the other hand, in the case of PIr, without SOC, the band structure exhibits similar Kagome features (e.g., flat bands, Dirac-like crossings), but the bands are more dispersive than in PCa_2, indicating stronger hybridization or overlap between orbitals, likely due to Ir's more extended 5d orbitals. When SOC is added, there is a clear lifting of degeneracies and visible band splittings, especially near the Fermi level. These effects stem from the strong SOC in Ir, which is a heavy element. **Figure 5** presents the electronic Figure 5 illustrates the electronic consequencess of these structural differences, demonstrating the band dispersions of PCa$_2$ and PIr. This is noted by looking into the band dispersions of PCa$_2$ and PIr, highlighting the differing effects of spin-orbit coupling. In PCa$_2$, the almost degenerate flat bands (strong electron localization) shows the small relativistic nature of Ca and the continuation of the Kagome lattice. Conversely, in PIr, the significant SOC effects of Ir generate splitting of several degeneracies, leading to asymmetric gaps along high-symmetry paths. Therefore, chiral symmetry is able to incorporate the physics of both light and heavy elements, providing a flexible pathway from nearly perfect Kagome flat-band characteristics to spin-orbit-induced topological band splitting. The splitting may open small gaps at symmetry-protected points, which could have implications for topological states (e.g., quantum spin Hall effect or chiral edge states in layered structures).

A central observation from our analysis is the role of atomic size and charge in dictating Wyckoff site occupation, particularly in the context of the 3d site responsible for forming Kagome planes. We find that small, moderately charged cations—those with

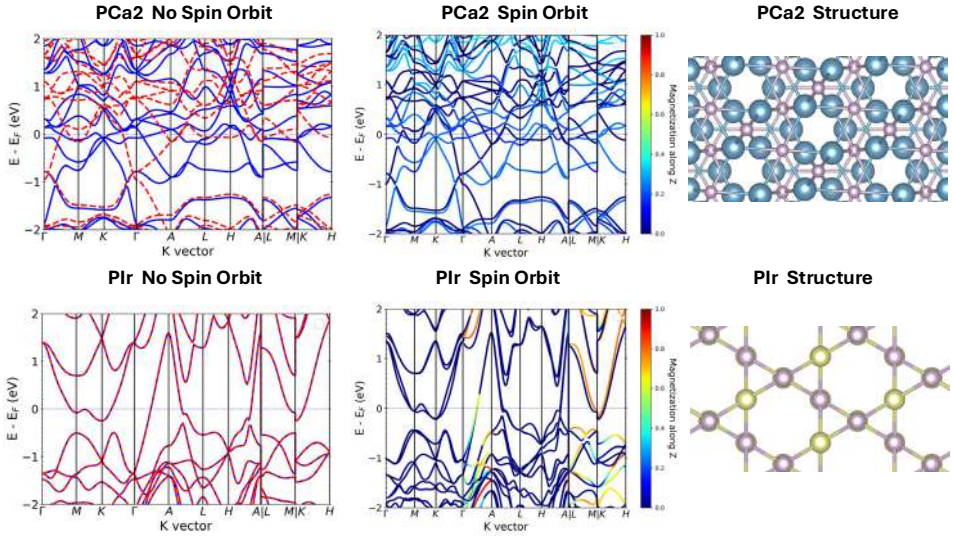

Figure 5. Electronic band structures of two representative compounds identified in our structural search. The top row corresponds to PCa_2 and the bottom row to PIr. In both cases, phosphorus occupies the 3d Wyckoff position, forming the Kagome network. However, Ca resides in the 6j site in PCa_2, while Ir occupies the 3c site in PIr, leading to distinct coordination environments. These differences are further amplified by the oxidation states and spin-orbit coupling (SOC) effects. As expected, SOC has minimal impact in the Ca-based compound, while in PIr, SOC induces significant band splitting and lifts degeneracies along multiple high-symmetry directions. Despite these contrasts, both systems preserve the hallmark hexagonal dispersion associated with P at the 3d site, underscoring the structural role of phosphorus in stabilizing the Kagome lattice.

Revista de la Academia Colombiana de Ciencias Exactas, Físicas y Naturales
49(193):714-727, octubre-diciembre de 2025. doi: https://doi.org/10.18257/raccefyn.3256

Shannon radii typically below 0.6 Åand oxidation states of +2 or +3—are far more likely to occupy the 3d site. This is not surprising when considering the geometric constraints of the Kagome motif, which requires near-planarity and tight angular coordination. What stands out, however, is the consistency of this trend across diverse chemistries: elements like Be^{2+}, As^{3+}, and Cd^{2+} dominate 3d site occupations, while the same species are rarely found at sites like 3c or 6j unless steric balance demands it. These preferences likely reflect a balance between crystal field stability and efficient packing, a hypothesis supported by formation energy data in the Materials Project and ICSD entries. In this way, the dataset provides empirical support for the idea that chiral Kagome materials enforce both spatial and electrostatic selectivity in their site chemistry.

The comparison of band structures between Ca- and Ir-containing compounds further reveals how these local structural environments shape magnetic order. Both systems were initialized with a ferromagnetic configuration, yet they relaxed to different magnetic ground states. The Ca-based compound (P3d.Ca6j) retained a net ferromagnetic signature, evident in the clean, asymmetric splitting of the spin bands and the absence of band folding. The Ir-based system (P3d.Ir3c), however, showed clear evidence of symmetry breaking: the bands split in a staggered fashion with doubling along key symmetry lines, consistent with an antiferromagnetic or ferrimagnetic solution. These divergences, despite similar symmetry and stoichiometry, highlight a delicate competition between exchange interactions, local coordination geometry, and perhaps even subtle differences in orbital overlap. Importantly, the preservation of enantiomorphic symmetry in both cases (space group 180) suggests that these materials could still host topologically nontrivial states—particularly if spin-orbit coupling or external perturbations are introduced. These results underscore how even minor changes in site occupancy and elemental identity can lead to qualitatively different electronic and magnetic behavior within the same structural framework.

Conclusions

We have developed a framework for identifying and analyzing chiral Kagome materials in space group 180 using a combination of Shannon radii, oxidation states, and Wyckoff position analysis. Our data reveal clear trends linking cation size and charge to the structural role within the Kagome motif, with elements like Be^{2+}, As^{3+}, and Cd^{2+} dominating the high-symmetry 3d site. Comparative electronic structure analysis of P3d.Ca6j and P3d.Ir3c compounds reveals sensitivity to magnetic ordering despite identical symmetry and stoichiometry, indicating complex interdependencies between the local atomic environment and emergent quantum states.

These insights offer concrete design guidelines for the discovery of next-generation Kagome systems with topological and magnetic functionalities. Beyond providing structural descriptors, our results suggest that magnetic ground states and band topology can be finely tuned by targeted control of atomic size, charge, and coordination environment. This approach paves the way for the rational design of new materials that may rival or exceed the electronic richness of canonical Kagome metals such as Fe_3Sn_2 and CoSn.

Acknowledgments

Computational resources have been provided by the Pittsburgh Supercomputer Center (Bridges2) and San Diego Supercomputer Center (Expanse) through allocation DMR140031 from the Advanced Cyberinfrastructure Coordination Ecosystem: Services & Support (ACCESS) program, which is supported by National Science Foundation grants #2138259, #2138286, #2138307, #2137603, and #2138296. We acknowledge the computational resources provided by WVU Research Computing's Dolly Sods HPC cluster, partially supported by NSF grant OAC-2117575. Additionally, we are grateful for funding from the West Virginia Higher Education Policy Commission under the Research Challenge Grant Program 2022 (Award RCG 23-007) and the NASA EPSCoR Program (Award 80NSSC22M0173).

References

Ardila-Gutiérrez, C., Torres-Amaris, D., González-Hernández, R., Romero, A.H., & Garcia-Castro, A. (2025). Chiral symmetry and magnetism in a 3d kagome lattice: RPt$_2$B b (r= la and nd) prototype crystals. *Physical Review B 112, 035109 (2025)*

Bousquet, E., Fava, M., Romestan, Z., Gómez-Ortiz, F., McCabe, E. E., & Romero, A. H. (2024). Structural chirality and related properties in the periodic inorganic solids: Review and perspectives. *Journal of Physics: Condensed Matter*, *37*(16), 163004.

Chen, C., & Ong, S. P. (2022). A universal graph deep learning interatomic potential for the periodic table. *Nature Computational Science*, *2*(11), 718-728.

Chen, H., Wu, W., Yang, S. A., Li, X., & Zhang, L. (2019). Chiral phonons in kagome lattices. *Physical Review B*, *100*(9), 094303.

Choudhary, K., Garrity, K. F., Reid, A. C., DeCost, B., Biacchi, A. J., Hight Walker, A. R., Trautt, Z., Hattrick-Simpers, J., Kusne, A., Centrone, A., Davydov, A., Jiang, J., Pachter, R., Cheon, G., Reed, E., Agrawal, A., Qian, X., Sharma, V., ..., Rabe, K., & Tavazza, F. (2020). The joint automated repository for various integrated simulations (jarvis) for data-driven materials design. *npj computational materials*, *6*(1), 173.

Choudhary, K., Wines, D., Li, K., Garrity, K. F., Gupta, V., Romero, A. H., Krogel, J. T., Saritas, K., Fuhr, A., Ganesh, P., Kent, P. R. C., Yan, K. , Lin, Y.., Ji, S., Blaiszik, B. , Reiser, P., Friedrich, P., Agrawal, A., Tiwary, P., ..., Biachi, A.J., & Tavazza, F. (2024). Jarvis-leaderboard: A large scale benchmark of materials design methods. *npj Computational Materials*, *10*(1), 93.

Curtarolo, S., Setyawan, W., Hart, G. L., Jahnatek, M., Chepulskii, R. V., Taylor, R. H., Wang, S., Xue, J., Yang, K., Levy, O., Mehl, M.J., Stokes, H.T., Demchenko, D.O., & Morgan, D. (2012). Aflow: An automatic framework for high-throughput materials discovery. *Computational Materials Science*, *58*, 218-226.

Elliott, R. J. (1961). Phenomenological discussion of magnetic ordering in the heavy rare-earth metals. *Physical Review*, *124*(2), 346.

Fredericks, S., Parrish, K., Sayre, D., & Zhu, Q. (2021). Pyxtal: A python library for crystal structure generation and symmetry analysis. *Computer Physics Communications*, *261*, 107810.

Fu, J., Han, Y., Wang, Y., Wu, H., Yang, Y., Du, R., Zhao, J., Zhang, H., Yu, J., Wang, Z., & Hu, J. (2025). Ultrafast coherent phonon dynamics in the kagome magnet GdV$_6$Sn$_6$. *Physical Review B*, *111*(5), 054308.

Hasan, M. Z., Chang, G., Belopolski, I., Bian, G., Xu, S.-Y., & Yin, J.-X. (2021). Weyl, dirac and high-fold chiral fermions in topological quantum matter. *Nature Reviews Materials*, *6*(9), 784-803.

Hasan, M. Z., Xu, S.-Y., Belopolski, I., & Huang, S.-M. (2017). Discovery of weyl fermion semimetals and topological fermi arc states. *Annual Review of Condensed Matter Physics*, *8*(1), 289-309.

Herath, U., Tavadze, P., He, X., Bousquet, E., Singh, S., Muñoz, F., & Romero, A. H. (2020). Pyprocar: A python library for electronic structure pre/post-processing. *Computer Physics Communications*, *251*, 107080.

Hu, Y., Ma, J., Li, Y., Jiang, Y., Gawryluk, D. J., Hu, T., Teyssier, J., Multian, V., Yin, Z., Xu, S., Shin, S., Plokhikh, I., Han, X., Plumb, N.C., Liu, Y.., Yin, J.-X., Guguchia, Z., Zhao, Y., Schnyder, A.P., ...,Wang, N., & Shi, M. (2024). Phonon promoted charge density wave in topological kagome metal ScV$_6$Sn$_6$. *Nature communications*, *15*(1), 1658.

Ivantchev, S., Kroumova, E., Madariaga, G., Pérez-Mato, J., & Aroyo, M. (2000). Subgroupgraph: A computer program for analysis of group–subgroup relations between space groups. *Applied Crystallography*, *33*(4), 1190-1191.

Jain, A., Montoya, J., Dwaraknath, S., Zimmermann, N. E., Dagdelen, J., Horton, M., Huck, P., Winston, D., Cholia, S., Ong, S. P. & Persson, K. (2020). The materials project: Accelerating materials design through theory-driven data and tools. *Handbook of Materials Modeling: Methods: Theory and Modeling*, 1751-1784.

Jain, A., Ong, S. P., Hautier, G., Chen, W., Richards, W. D., Dacek, S., Cholia, S., Gunter, D., Skinner, D., Ceder, G. & Persson, K. (2013). Commentary: The materialsproject: A materials genome approach to accelerating materials innovation. *APL materials*, *1*(1).

Kaplan, T. (1961). Some effects of anisotropy on spiral spin-configurations with application to rare-earth metals. *Physical Review*, *124*(2), 329.

Kazeev, N., Nong, W., Romanov, I., Zhu, R., Ustyuzhanin, A., Yamazaki, S., & Hippalgaonkar, K. (2025). Wyckoff transformer: Generation of symmetric crystals. *arXiv preprint arXiv:2503.02407*.

Kresse, G., & Furthmüller, J. (1996). Efficiency of ab-initio total energy calculations for metals and semiconductors using a plane-wave basis set. *Computational materials science*, *6*(1), 15-50.

Kresse, G., & Hafner, J. (1993). Ab initio molecular dynamics for liquid metals. *Physical review B*, *47*(1), 558.

Kresse, G., & Hafner, J. (1994). Norm-conserving and ultrasoft pseudopotentials for first-row and transition elements. *Journal of Physics: Condensed Matter*, *6*(40), 8245.

Kresse, G., & Joubert, D. (1999). From ultrasoft pseudopotentials to the projector augmented-wave method. *Physical review b*, *59*(3), 1758.

Laboratory, L. A. N. (2025). Periodic table of elements: Lanl [Accessed: 2025-07-10]. Lang, L., Tavadze, P., Tellez, A., Bousquet, E., Xu, H., Muñoz, F., Vasquez, N.,

Lang, L, Tavadze, P., Tellez, A., Bousquet, E., Xu, H., Muñoz, F., Vasquez, N., Herath, U., & Romero, A.H. (2024). Expanding pyprocar for new features, maintainability, and reliability. *Computer Physics Communications*, *297*, 109063.

Li, J., Yao, Q., Wu, L., Hu, Z., Gao, B., Wan, X., & Liu, Q. (2022). Designing light-element materials with large effective spin-orbit coupling. *Nature Communications*, *13*(1), 919.

Liu, M., & Meng, S. (2024). Recent breakthrough in ai-driven materials science: Tech giants introduce groundbreaking models. *arXiv preprint arXiv:2402.05799*.

Liu, Z., Li, M., Wang, Q., Wang, G., Wen, C., Jiang, K., Lu, X., Yan, S., Huang, Y., Shen, D., Yin, J.X., Wang, Z., Yin, Z., Lei, H., & Wang, S. (2020). Orbital-selective dirac fermions and extremely flat bands in frustrated kagome-lattice metal CoSn. *Nature communications*, *11*(1), 4002.

Mekata, M. (2003). Kagome: The story of the basketweave lattice. *Physics Today*, *56*(2), 12-13.

Merchant, A., Batzner, S., Schoenholz, S. S., Aykol, M., Cheon, G., & Cubuk, E. D. (2023). Scaling deep learning for materials discovery. *Nature*, *624*(7990), 80-85.

Momma, K., & Izumi, F. (2011). Vesta 3 for three-dimensional visualization of crystal, volumetric and morphology data. *Applied Crystallography*, *44*(6), 1272-1276.

Nakatsuji, S., Kiyohara, N., & Higo, T. (2015). Large anomalous hall effect in a non-collinear antiferromagnet at room temperature. *Nature*, *527*(7577), 212-215.

Negi, P., Medhi, K., Pancholi, A., & Roychowdhury, S. (2025). Magnetic kagome materials: Bridging fundamental properties and topological quantum applications. *Materials Horizons*.

Newnham, R. E. (2004). *Properties of materials: Anisotropy, symmetry, structure*. OUP Oxford.

Ortiz, B. R., Teicher, S. M., Hu, Y., Zuo, J. L., Sarte, P. M., Schueller, E. C., Abeykoon, A. M., Krogstad, M. J., Rosenkranz, S., Osborn, R., Seshadri, R., Balents, L., He, J., & Wilson, S.D. (2020). CsV$_3$Sb$_5$: A \mathcal{Z}_2 topological kagome metal with a superconducting ground state. *Physical Review Letters*, *125*(24), 247002.

Powell, R. C., & Powell, R. C. (2010). Tensor properties of crystals. *Symmetry, Group Theory, and the Physical Properties of Crystals*, 55-78.

Prakash, A., & Wei, T.-C. (2014). Ground states of 1d symmetry-protected topological phases and their utility as resource states for quantum computation. *arXiv preprint arXiv:1410.0974*.

Saini, H. (2023). *Development of ab initio characterization tool for weyl semimetals and thermodynamic stability of kagome weyl semimetals.* [Doctoral dissertation].

Schmidt, J., Cerqueira, T. F., Romero, A. H., Loew, A., Jäger, F., Wang, H.-C., Botti, S., & Marques, M. A. (2024). Improving machine-learning models in materials science through large datasets. *Materials Today Physics*, *48*, 101560.

Tasci, E., de la Flor, G., Orobengoa, D., Capillas, C., Perez-Mato, J., & Aroyo, M. (2012). An introduction to the tools hosted in the bilbao crystallographic server. *EPJ Web of Conferences*, *22*, 00009.

Toulouse, G. (2008). The frustration model. In *Modern trends in the theory of condensed matter: Proceedings of the xvi karpacz winter school of theoretical physics, february 19–march 3, 1979 karpacz, poland* (pp. 195-203). Springer.

Wang, Q., Lei, H., Qi, Y., & Felser, C. (2024). Topological quantum materials with kagome lattice. *Accounts of Materials Research*, *5*(7), 786-796.

Wannier, G. (1950). Antiferromagnetism. the triangular ising net. *Physical Review*, *79*(2), 357.

Xie, T., & Grossman, J. C. (2018). Crystal graph convolutional neural networks for an accurate and interpretable prediction of material properties. *Physical review letters*, *120*(14), 145301.

Ye, L., Kang, M., Liu, J., Von Cube, F., Wicker, C. R., Suzuki, T., Jozwiak, C., Bostwick, A., Rotenberg, E., Bell, D. C., Fu, L., Comin, R., & Checkelsky, J.G. (2018). Massive dirac fermions in a ferromagnetic kagome metal. *Nature*, *555* (7698), 638-642.

Yin, J.-X., Lian, B., & Hasan, M. Z. (2022). Topological kagome magnets and superconductors. *Nature*, *612*(7941), 647-657.

Yoshimori, A. (1959). A new type of antiferromagnetic structure in the rutile type crystal. *Journal of the Physical Society of Japan*, *14*(6), 807-821.

You, J.-Y., Zhou, X., Hou, T., Yahyavi, M., Jin, Y., Hung, Y.-C., Singh, B., Zhang, C., Yin, J.-X., Bansil, A. & Chang, G. (2023). Topological chiral kagome lattice. *arXiv preprint arXiv:2309.00217*.

Zhang, C.-L., Liang, T., Bahramy, M., Ogawa, N., Kocsis, V., Ueda, K., Kaneko, Y., Kriener, M., & Tokura, Y. (2021). Berry curvature generation detected by nernst responses in ferroelectric weyl semimetal. *Proceedings of the National Academy of Sciences*, *118*(44), e2111855118.

Zhou, L., Yang, F., Zhang, S., & Zhang, T. (2024). Chemical rules for stacked kagome and honeycomb topological semimetals. *Advanced Materials*, *36*(15), 2309803.

Zhu, R., Nong, W., Yamazaki, S., & Hippalgaonkar, K. (2024). Wycryst: Wyckoff inorganic crystal generator framework. *Matter*, *7*(10), 3469-3488.